

Quantum tomography as a tool for the characterization of optical devices

G Mauro D'Ariano¹, Martina De Laurentis², Matteo G A Paris¹,
Alberto Porzio^{2,3} and Salvatore Solimeno^{2,3}

¹ Quantum Optics and Information Group, Unità INFN and Università di Pavia, via Bassi 6, I-27100 Pavia, Italy

² Dipartimento di Scienze Fisiche, Università 'Federico II', Complesso Universitario di Monte Sant'Angelo, via Cintia, 80126 Napoli, Italy

³ INFN Unità di Napoli, Italy

Received 19 November 2001

Published 27 March 2002

Online at stacks.iop.org/JOptB/4/S127

Abstract

We describe a novel tool for the quantum characterization of optical devices. The experimental set-up involves a stable reference state that undergoes an unknown quantum transformation and is then revealed by balanced homodyne detection. Through tomographic analysis of the homodyne data we are able to characterize the signal and to estimate parameters of the interaction, such as the loss of an optical component or the gain of an amplifier. We present experimental results for coherent signals, with application to the estimation of losses introduced by simple optical components, and show how these results can be extended to the characterization of more general optical devices.

Keywords: Quantum tomography, optical devices, homodyne detection

1. Introduction

Quantum homodyne tomography (QHT) is certainly the most successful technique for measuring the quantum state of radiation. It is based on homodyne detection, where the signal mode is amplified by the local oscillator. This means that there is no need for single-photon resolving photodetectors, whence it is possible to achieve quantum efficiency η approaching the ideal unit value by using linear photodiodes [1]. Moreover, QHT is efficient and statistically reliable, such that it can be used on-line with the experiment. Indeed, among other proposed state reconstruction methods, QHT is the only one which has been implemented in quantum optical experiments [2, 3].

Possible applications of QHT range from the measurement of photon correlations on a subpicosecond time-scale [2] to the characterization of squeezing properties [3, 4], photon statistics in parametric fluorescence [5], quantum correlations in down-conversion [1] and non-classicality of states [6]. In general, the key point is that QHT provides information about the quantum state within a chosen sideband, thus allowing precise spectral characterization of the light beam under investigation.

In this paper we address QHT as a tool for quantum characterization of optical devices, as in the estimation of the coupling constant of an active medium or the quantum efficiency of a photodetector. The goal is to link the estimation of such parameters with the results from feasible measurement schemes, such as homodyne detection, and to make the estimation procedure as efficient as possible. We present our experimental results for the reconstruction of the quantum state of coherent signals, together with application to the estimation of the losses introduced by simple optical components. Moreover, we show how these preliminary results can be extended to the characterization of more general optical devices.

In the next section we review some basic elements of quantum tomography, and in section 3 we describe the basic requirements needed to implement a quantum characterization tool based on tomographic measurements. In section 4 the experimental apparatus is described with some details, and in section 5 the experimental data are analysed and discussed. Section 6 closes the paper by discussing the possible extensions of the present work.

2. Quantum homodyne tomography

Quantum tomography of a single-mode radiation field consists of a set of repeated measurements of the field-quadrature $x_\phi = \frac{1}{2}(ae^{-i\phi} + a^\dagger e^{i\phi})$ at different values of the reference phase ϕ . The expectation value of a generic operator can be obtained by averaging a suitable kernel function $R[O](x, \phi)$ as follows [7]

$$\text{Tr}\{\rho O\} = \int_0^\pi \frac{d\phi}{\pi} \int_{-\infty}^{\infty} dx p(x, \phi) R[O](x, \phi) \quad (1)$$

where $p(x, \phi)$ denotes the probability distribution of the outcomes x for the quadrature x_ϕ , and $R[O](x, \phi)$ is given by

$$R[O](x, \phi) = \frac{1}{4} \int_0^\infty dr \text{Tr}\{O \cos[\sqrt{r}(x - x_\phi)]\}. \quad (2)$$

Actually, the tomographic kernel $R[O](x, \phi)$ for a given operator O is not unique, since a large class of *null functions* [9, 10] $F(x, \phi)$ exists that have zero tomographic average for an arbitrary state. This degree of freedom can be exploited to *adapt* the kernel to data and achieve an optimized determination of the quantity of interest. For example, quantities like the photon number, the field amplitude and any normally ordered moment can be tomographically estimated by averaging the following kernel

$$K[O](x, \phi) = R[O](x, \phi) + \sum_{k=0}^{M-1} \mu_k F_k(x, \phi) + \sum_{k=0}^{M-1} \mu_k^* F_k^*(x, \phi) \quad (3)$$

where the kernels $R[O]$ for the moments are given by [11]

$$R[a^{\dagger n} a^m](x; \phi) = e^{i(m-n)\phi} \frac{H_{n+m}(\sqrt{2}x)}{\sqrt{2^{n+m} \binom{n+m}{n}}} \quad (4)$$

$H_n(x)$ being the Hermite polynomial of order n , and the null functions F_k are expressed as $F_k(x, \phi) = x^k e^{i(k+2)\phi}$, $k = 0, 1, \dots$. The coefficients μ_k are obtained by minimizing the rms error for the given kernel on the given homodyne sample. A similar approach can be applied to optimize the reconstruction of the matrix elements $\rho_{mn} = \langle m|\rho|n\rangle$, thus achieving an effective quantum state characterization.

3. QHT as a tool for estimating parameters

The state reconstruction method provided by QHT is effective and reliable, such that it can be exploited to build a tool to characterize quantum devices. The general scheme for such a tool should be as follows. First, we need a stable source of quantum states, i.e. a source able to provide repeated preparations of a reference signal. The signal can be characterized by QHT, and then employed as the input to a given device which we want to characterize by the estimation of some relevant parameters. At the output, the transformed state can be analysed by QHT, so as to characterize the input–output relations of the device.

In order to implement this kind of scheme two basic requirements should be satisfied: (i) we need a stable source for the reference signal; (ii) effective data processing for the

tomographic samples should be devised, in order to minimize the number of measurements.

The first point can be satisfied by considering Gaussian signals, like coherent or squeezed states. Indeed, quantum signals that are most likely to be reliably generated in a laboratory are Gaussian states. The most general Gaussian state can be written as $\rho = D(\mu) S(r) \nu S^\dagger(r) D^\dagger(\mu)$, where ν denotes a thermal state $\nu = (n_{th} + 1)^{-1} [n_{th}/(n_{th} + 1)]^{a^\dagger a}$, $S(r) = \exp[r(a^2 - a^{\dagger 2})/2]$ the squeezing operator and $D(\mu) = \exp(\mu a^\dagger - \mu^* a)$ the displacement operator. However, thermal excitations can be neglected at optical frequencies, such that we may generally consider ν as the vacuum state. The homodyne distribution of the state ρ at phase ϕ with respect to the local oscillator is Gaussian and, remarkably, such Gaussian character is not altered by many transformations induced by optical devices, such as the loss of a component, the gain of an amplifier or the quantum efficiency of a detector. In this paper we consider the reference signal excited in a coherent state. More general signals will be considered elsewhere.

The need for effective data processing leads us to consider the use of either adaptive or maximum-likelihood (ML) procedures with the tomographic data. In section 5 we apply adaptive tomography for the estimation of losses induced by optical filters. Here we illustrate the use of an ML procedure for the characterization of a general (active or passive) optical medium, which we plan to perform experimentally in the near future.

Let us start by reviewing the ML approach. Let $p(x|\lambda)$ be the probability density of a random variable x , conditioned to the value of the parameter λ . The analytical form of p is known, but the true value of the parameter λ is unknown, and should be estimated from the result of a measurement of x . Let x_1, x_2, \dots, x_N be a random sample of size N . The joint probability density of the independent random variable x_1, x_2, \dots, x_N (the global probability of the sample) is given by

$$\mathcal{L}(\lambda) = \prod_{k=1}^N p(x_k|\lambda) \quad (5)$$

and is called the likelihood function of the given data sample. The ML estimator of the parameter λ is defined as the quantity λ_{ML} that maximizes $\mathcal{L}(\lambda)$ for variations of λ . Since the likelihood is positive this is equivalent to maximizing

$$L(\lambda) = \log \mathcal{L}(\lambda) = \sum_{k=1}^N \log p(x_k|\lambda) \quad (6)$$

which is the so-called log-likelihood function.

Let us consider a generic optical medium: the propagation of a signal is governed, for negligible saturation effects, by the master equation

$$\dot{\rho} = G_1 L[a]\rho + G_2 L[a^\dagger]\rho \quad (7)$$

where ρ is the density matrix describing the quantum state of the signal mode a and $L[O]$ denotes the Lindblad superoperator $L[O]A = O A O^\dagger - \frac{1}{2} O^\dagger O A - \frac{1}{2} A O^\dagger O$. If we model the propagation as the interaction of a travelling wave single-mode a with a system of N identical two-level atoms, then the absorption parameter $G_1 = \gamma N_1$ and the amplification parameter $G_2 = \gamma N_2$ are related to the number

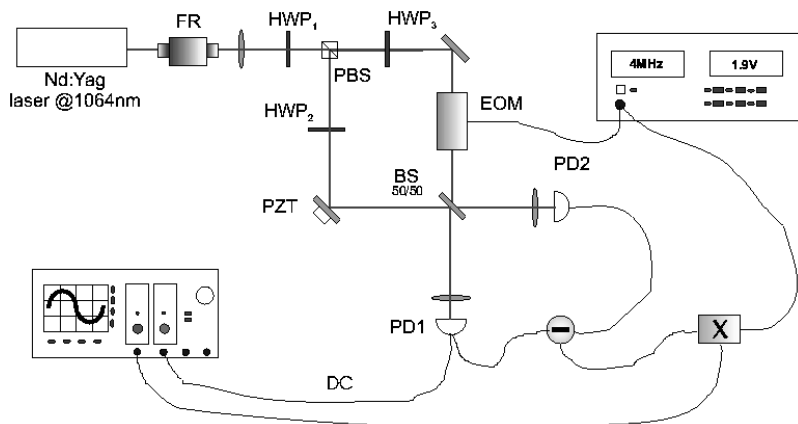


Figure 1. Schematic diagram of the experimental set-up. A Nd:YAG laser beam is divided into two beams, one acts as the homodyne local oscillator and the other represents the signal beam. The signal is modulated at frequency Ω with a defined modulation depth to control the average photon number in the generated coherent state. The tomographic data are provided by a homodyne detector whose difference photocurrent is demodulated and then acquired by a digital oscilloscope (Tektronix TDS 520D).

N_1 and N_2 of atoms in the lower and upper level respectively. The quantity γ is a rate of the order of the atomic linewidth [12], and the propagation gain (or deamplification) is given by $\mathcal{G} = \exp[(G_2 - G_1)t]$. A medium described by the master equation (7) represents a kind of phase-insensitive optical device, such that the parameters G_1 and G_2 can be estimated starting from random phase tomographic data. According to (7), the homodyne distribution of a coherent signal with initial amplitude α_0 is given, after the propagation, by

$$p(x; \phi) = \frac{1}{\sqrt{\pi(\delta^2 + g^2/2)}} \times \exp\left(-\frac{1}{\delta^2 + g^2/2} [x - g\text{Re}(\alpha_0 e^{-i\phi})]^2\right) \quad (8)$$

with $g = e^{-Q_t}$, $2Q = (G_1 - G_2)$, and $\delta^2 = (G_1 + G_2)(1 - g^2)/4Q$ (for non-unit quantum efficiency $\eta < 1$, $\delta^2 + g^2/2 \rightarrow \delta^2 + g^2/2 + (1 - \eta)/2\eta$). By ML estimation on homodyne data we may reconstruct the parameters G_1 and G_2 . The resulting method has been shown to be efficient by numerical simulations [13], and provides a precise determination of the absorption and amplification parameters of the master equation using a small homodyne data sample. Notice that no advantage should be expected in using squeezed states, because of the phase-insensitive character of the device.

4. Experimental details

A schematic diagram of the experiment is presented in figure 1. The principal radiation source is provided by a monolithic Nd:YAG laser (≈ 50 mW at 1064 nm; Lightwave, model 142). The laser has a linewidth of less than 10 kHz ms^{-1} with a frequency jitter of less than 300 kHz s^{-1} , while its intensity spectrum is shot-noise limited above 2.5 MHz. The laser emits a linearly polarized beam in a TEM₀₀ mode.

The laser is protected from back reflection by a Faraday rotator (FR) whose output polarizing beamsplitter can be adjusted to obtain an output beam of variable intensity. The beam leaving the isolator, of ≈ 2.5 mW, is then split into two parts of variable relative intensity by a combination of a halfwave plate (HWP₁) and a polarizing beamsplitter (PBS,

p-transmitted, s-reflected). The strongest part is sent directly toward the homodyne beamsplitter (BS) where it acts as the local oscillator beam. One of the mirrors in the local oscillator path is piezo mounted to obtain a variable phase difference between the two beams. The remaining part, typically less than 200 μW , is the homodyne signal. The optical paths travelled by the local oscillator and the signal beams are carefully adjusted to obtain a visibility typically above 75% measured at one of the homodyne output ports. The signal beam is modulated by means of a phase electro-optic modulator (EOM, Linos Photonics PM0202) at 4 MHz, and a halfwave plate (HWP₂, HWP₃) is mounted in each path to carefully match the polarization state at the homodyne input.

The basic property of the homodyne detector (described in detail in [15]) is the narrow-band detection of the field fluctuations around 4 MHz. The detector is composed by a 50/50 beamsplitter (BS), two amplified photodiodes (PD1, PD2) and a power combiner. The difference photocurrent is demodulated at 4 MHz by means of an electrical mixer. In this way the detection occurs outside any technical noise and, more importantly, in a spectral region where the laser does not carry excess noise.

The phase modulation added to the signal beam moves a certain number of photons, proportional to the square of the modulation depth, from the carrier optical frequency ω to the side bands at $\omega \pm \Omega$ so generating two few-photon coherent states, with an engineered average photon number, at frequencies $\omega \pm \Omega$. The sum of the sideband modes is then detected as a controlled perturbation attached to the signal beam [3]. The demodulated current is acquired by a digital oscilloscope (Tektronix TDS 520D) with 8-bit resolution and a record length of 250 000 points per run. The acquisition is triggered by a triangular shaped waveform applied to the piezo-electric (PZT) mounted on the local oscillator path. The piezo ramp is adjusted to obtain a 2π phase variation between the local oscillator and the signal beam in an acquisition window.

The homodyne data to be used for tomographic reconstruction of the radiation state have been calibrated according to the noise of the vacuum state. This is obtained by acquiring a set of data leaving the signal beam undisturbed

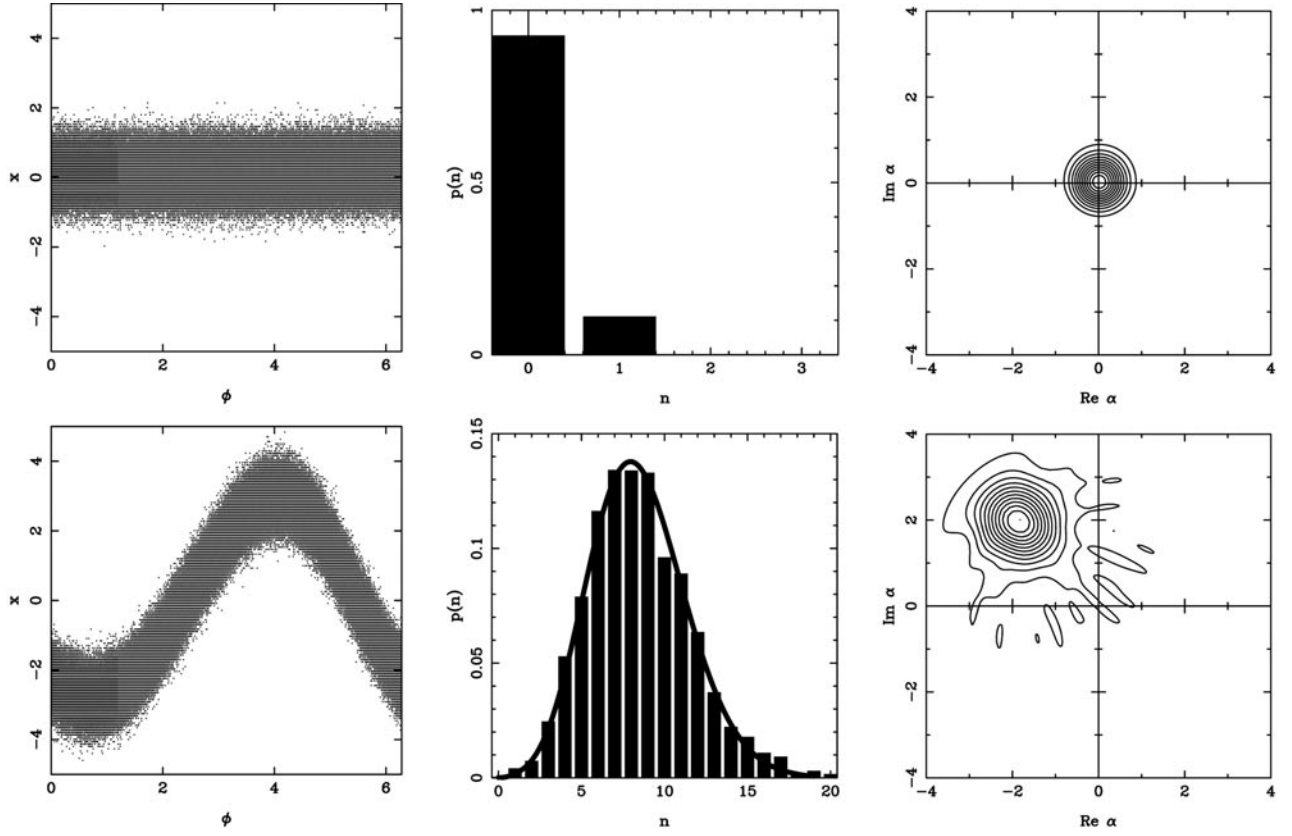


Figure 2. Reconstruction of the quantum state of the signal, and of the vacuum state used for calibration. For both states, from left to right, we report the raw data, a histogram of the photon number distribution and a contour plot of the Wigner function. Reconstruction has been performed for a sample of $N = 242\,250$ homodyne data. The coherent signal has an estimated average photon number equal to $\langle a^\dagger a \rangle = 8.4$. The solid line denotes the theoretical photon distribution of a coherent state with that number of photons. Statistical errors on matrix elements are about 2%. The slight phase asymmetry in the Wigner distribution corresponds to a value of about the 2% of the maximum.

while scanning the local oscillator phase. It is important to note that in case of the vacuum state no role is played by the visibility at the homodyne BS.

5. Data analysis

Our tomographic samples consist of N homodyne data $\{x_j, \phi_j\}_{j=1, \dots, N}$ with phases ϕ_j equally spaced with respect to the local oscillator. Since the piezo ramp is active during the whole acquisition time, we have a single value x_j for any phase ϕ_j . From calibrated data we first reconstruct the quantum state of the homodyne signal. According to the experimental set-up described in the previous section we expect a coherent signal with nominal amplitude that can be adjusted by varying the modulation depth of the optical mixer. However, since we do not compensate for the quantum efficiency of photodiodes in the homodyne detector ($\eta \simeq 90\%$) we expect to reveal coherent signals with reduced amplitude with respect to the actual one. In addition, the amplitude is further reduced by the non-maximum visibility (ranging from 75 to 85%) at the homodyne BS.

In figure 2 we show a typical reconstruction, together with the reconstruction of the vacuum state used for calibration. For both states, we report the raw data, the photon number distribution, i.e. the diagonal elements $Q_{nn} \equiv \langle n|Q|n \rangle$ of the density matrix in the Fock representation, and a contour plot

of the Wigner function. The matrix elements are obtained by sampling the corresponding kernel functions

$$R[|n\rangle\langle n+k|](x, \phi) = 2 \exp(-ik\phi) \sqrt{2^k n!(n+k)!} f_{nk}(x)$$

where

$$f_{nk}(x) = \begin{cases} \sum_{l=0}^n \frac{(-)^l 2^l \Gamma(1+l+k/2)}{l!(n-l)!(l+k)!} \\ \times \Phi(1+l+k/2, 1/2; -2x^2) & k \text{ even} \\ \sum_{l=0}^n \frac{(-)^l 2^{l+1/2} \Gamma(1+l+(k+1)/2)}{l!(n-l)!(l+k)!} 2xe^{-2x^2} \\ \times \Phi(-l-k/2, 3/2; 2x^2) & k \text{ odd} \end{cases}$$

and $\Phi(a, b; x)$ denotes a confluent hypergeometric function. The tomographic determination of the matrix elements is given by the averages

$$Q_{nk} = \overline{R[|n\rangle\langle k|]} = \frac{1}{N} \sum_j R[|n\rangle\langle k|](x_j, \phi_j) \quad (9)$$

whereas the corresponding confidence intervals are given (for diagonal elements) by $\delta_{Q_{nn}} = \Delta Q / \sqrt{N}$, ΔQ being the rms deviation of the kernel R over data (for off-diagonal elements the confidence intervals are evaluated for the real and imaginary parts separately).

In order to see the quantum state as a whole, we also report the reconstruction of the Wigner function of the field, which is defined as follows

$$W(z) = \frac{2}{\pi} \text{Tr} \{ \varrho D(2z) (-)^{a^\dagger a} \} \quad (10)$$

and can be expressed in terms of the matrix elements as

$$W(z) = \text{Re} \sum_{d=0}^{\infty} e^{id\phi} \sum_{n=0}^{\infty} \Lambda(n, d; |z|^2) \rho_{n, n+d} \quad (11)$$

where

$$\Lambda(n, d; |z|^2) = (-)^n 2(2 - \delta_{d0}) |2z|^d \sqrt{\frac{n!}{(n+d)!}} e^{-2|z|^2} L_n^d(|2z|^2) \quad (12)$$

and $L_n^d(x)$ denotes the Laguerre polynomials. Of course, the series in equation (11) should be truncated at some point, and therefore the Wigner function can be reconstructed only at some finite resolution.

Once the coherence of the signal has been established we may use QHT to estimate the loss imposed by a passive optical component like an optical filter. The procedure may be outlined as follows. We first estimate the initial mean photon number $\bar{n}_0 = |\alpha_0|^2$ of the signal beam, and then the same quantity inserting an optical neutral density filter in the signal path. If Γ is the loss parameter, then the coherent amplitude is reduced to $\alpha_\Gamma = \alpha_0 e^{-\Gamma}$, and the intensity to $\bar{n}_\Gamma = \bar{n}_0 e^{-2\Gamma}$.

The estimation of the mean photon number can be performed adaptively on data by taking the average of the kernel

$$K[a^\dagger a](x) = 2x^2 - \frac{1}{2} + \mu e^{i2\phi} + \mu^* e^{-i2\phi} \quad (13)$$

where μ is a parameter to be determined in order to minimize fluctuations. As proved in [10] $\mu = -1/2\langle a^{\dagger 2} \rangle$, which itself can be obtained from homodyne data. In practice, one uses the data sample twice: first to evaluate μ , then to obtain the estimate for the mean photon number.

In figure 3 the tomographic determinations of \bar{n}_Γ are compared with the expected values for three sets of experiments, corresponding to three different initial amplitudes. The expected values are given by $\bar{n}_\Gamma = \bar{n}_0 e^{-2\Gamma} \mathcal{V}$, where Γ is the value obtained by comparing the signal dc currents I_0 and I_Γ at the homodyne photodiodes and $\mathcal{V} = V_\Gamma/V_0$ is the relative visibility. The full curves in figure 3 denote these values. The curves are not continuous due to variations of visibility. As is apparent from the plot, the estimation is reliable over the whole range of values which we could explore. It is worth noting that the present estimation is absolute, i.e. it does not depend on knowledge of the initial amplitude, and it is robust, since it may be performed independently of the quantum efficiency of the photodiodes employed for the homodyne detector.

One may note that the estimation of the loss can also be pursued by measuring an appropriate observable, typically the intensity of the light beam with and without the component. However, this is a concrete possibility only for high-amplitude signals, whereas losses on weakly excited coherent states cannot be properly characterized by direct photocounting using photodiodes (due to quantum efficiency and large fluctuations)

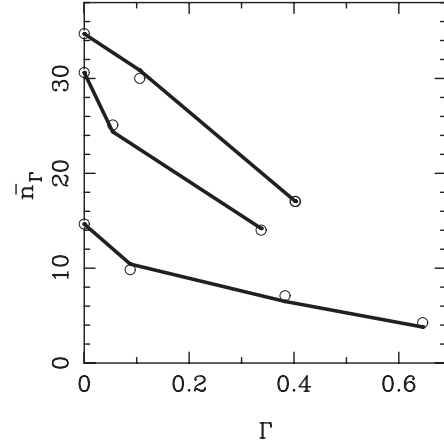


Figure 3. Estimation of the mean photon number of a coherent signal as a function of the loss imposed by an optical filter. Three sets of experiments, corresponding to three different initial amplitudes, are reported. Open circles are the tomographic determinations, whereas full curves denote the expected values, as follow from nominal values of loss and visibility at the homodyne detector. Statistical errors are within the circles.

or by avalanche photodetectors (due to the impossibility of discriminating between the numbers of photons). On the contrary, QHT provides the mean intensity (actually the whole photon distribution) independently of the excitation level of the signal, thus allowing a precise characterization in the quantum regime as well. Indeed, in [8] adaptive tomographic determination of the mean photon number has been extensively applied to (numerically simulated) homodyne data for coherent states of various amplitudes. The analysis has shown that the determination is also reliable for small samples and that precision is not affected by the intensity of the signal itself.

6. Conclusions and outlook

In this paper we investigated QHT as a tool for the characterization of quantum optical devices. We carried out quantum state reconstruction of coherent signals, and showed how QHT can be used to reliably estimate the loss imposed by an optical filter. We also show that the estimation procedure can be extended to the characterization of general (active or passive) optical devices, which we plan to perform experimentally in the near future. We also plan to extend our analysis to squeezed signals since it has been proved [14] that squeezing improves precision in the homodyne estimation of relevant parameters such as the phaseshift or the quantum efficiency of a photodetector. Moreover squeezed signals can be successfully employed to enhance the precision of the loss measurement procedure reported here. In particular, our aim is to reproduce the described measurement scheme at the output of an optical parametric oscillator cavity [16] driven below threshold to generate vacuum squeezed radiation.

Acknowledgment

This work has been sponsored by INFM under the project PAIS TWIN.

References

- [1] D'Ariano G M, Vasyliiev M and Kumar P 1998 *Phys. Rev. A* **58** 636
- [2] McAlister D F and Raymer M G 1997 *Phys. Rev. A* **55** R1609
- [3] Breitenbach G, Schiller S and Mlynek J 1997 *Nature* **387** 471
- [4] Breitenbach G and Schiller S 1997 *J. Mod. Opt.* **44** 2207
- [5] Fiorentino M, Conti A, Zavatta A, Giacomelli G and Marin F 2000 *J. Opt. B: Quantum Semiclass. Opt.* **2** 184
- [6] Vasyliiev M, Choi S-K, Kumar P and D'Ariano G M 1998 *Opt. Lett.* **23** 1393
- [7] D'Ariano G M, Sacchi M F and Kumar P 1999 *Phys. Rev. A* **59** 826
- [8] D'Ariano G M and Paris M G A 1999 *Phys. Rev. A* **60** 518
- [9] Opatrny T, Dakna M and Welsch D-G 1998 *Phys. Rev. A* **57** 2129
- [10] D'Ariano G M and Paris M G A 1998 *Acta Phys. Slovaca* **48**
- [11] Richter Th 1996 *Phys. Lett. A* **221** 327
- [12] Mandel L and Wolf E 1995 *Optical Coherence and Quantum Optics* (Cambridge: Cambridge University Press)
- [13] D'Ariano G M, Paris M G A and Sacchi M F 2001 *Quantum Communication, Computing, and Measurements* vol 3, ed P Tombesi and O Hirota (Dordrecht: Kluwer) p 155
- [14] D'Ariano G M, Paris M G A and Sacchi M F 2000 *Phys. Rev. A* **62** 023815
- [15] Porzio A, Sciarrino F, Chiummo A and Solimeno S 2001 *Opt. Commun.* **194** 373
- [16] Porzio A, Altucci C, Autiero M, Chiummo A, de Lisio C and Solimeno S 2001 *Appl. Phys. B* **73** 763–6